Third International Symposium on Marine Propulsors
smp'13, Launceston, Tasmania, Australia, May 2013

A Numerical Method for the Analysis of Unsteady Cavitating Rotor and Stator Interaction *

Ye Tian[1], Spyros A. Kinnas[2]

[1,2] Ocean Engineering Group, Department of Civil, Architectural and Environmental Engineering
The University of Texas at Austin, Austin, TX 78712, USA

ABSTRACT

A fully unsteady model to simulate the unsteady cavitating interactions of the rotor and stator propulsion system is proposed and implemented. The model includes three major components: an unsteady Vortex Lattice Method (VLM) model for the rotor, an unsteady Boundary Element Method (BEM) model for the stator, and a fully unsteady wake model for the rotor which can be applied with the obstruction of the downstream stator. The cavity model in the proposed methods in general was first validated for a single open propeller with the results from RANS simulation. Preliminary application of the current model was carried out on a test rotor and stator propulsion system without the hub and casing.

Keywords

Cavitation, Rotor and stator interaction, BEM.

1 INTRODUCTION

In recent years, rotor/stator propulsion systems have become very popular in the applications of high-speed commercial or navy watercrafts. The presence of the stator cancels the swirl velocity created by the rotor and thereby improves the efficiency of the propulsion system. Nevertheless, the analysis of the performance of the rotor/stator propulsion system brings into new challenges, due to the complexity of the geometric configuration and the intrinsic unsteadiness, which not only because of time-dependent relative motion between the rotor and stator, but also because of the unsteady wake of the rotor directly impinging onto the stator surface.

The numerical methods for the rotor and stator propulsion system can be classified into two types. The first type takes advantage of full-fledged viscous computational fluid dynamics (CFD) tools, such as Reynolds Averaged Navier-Stokes (RANS) solvers, or Large Eddy Simulation (LES) solvers. The other type makes use of potential flow methods including Vortex Lattice Method (VLM) and Boundary Element Method (BEM).

The viscous solvers contain more physical representations of the flow phenomena (e.g. flow separation, turbulence), and hence provides more flow information. However, fully viscous attack of the problem is significantly computational expensive, and require considerable effects of grid generation. Chun et al. (2002) study the unsteady rotor and stator interaction of a water-jet pump through RANS. Brewton et al. (2006) and Lindau et al. (2009, 2011) also carried out RANS simulation of a water-jet propulsor for fully wetted and cavitating cases in a circumferentially averaged sense.

The potential flow methods have been extensively used as tools for the design and analysis of marine propellers. Nonetheless, numerical difficulties arise from the treatment the distinct free wake sheets of the rotor when applying these methods to the rotor and stator interaction problem.

Taylor et al. (1998) and Kerwin et al. (2006) coupled VLM with RANS or Euler solver through body forces in order to analyze the global flow through a water-jet pump. Kinnas et al. (2007a, 2010) proposed an iterative steady model based on low order Boundary Element Method (BEM) for the rotor and stator interaction. In their model, the induced velocities from the rotor to the stator are averaged circumferentially, and vice versa. This model was extended by coupling with a boundary layer solver (Kinnas et al. 2007b). Michael et al. (2008) and Chesnakas et al. (2009) designed the ONR AxWJ-2 water-jet pump through VLM coupling with Euler solver, and evaluated the result of design, including the cavitating performance using RANS with a mixing-plane model, however, unsteady features of the problem were not addressed

RANS simulations of the unsteady interaction of the rotor and stator often apply a sliding interface (alternatively a RANS solver which allows overset grid could be a better option). The sliding interface, nonetheless, diffuses the rotor wake significantly, so that the corresponding numerical results could be questionable. On the other hand, potential flow methods with an unsteady wake model can describe the rotor wake in a more conservative way, although proper dissipation has to be introduced for this approach.

L. He (2010) presented a Vortex Lattice Method (VLM)/BEM model for the unsteady propeller and rudder interaction, which can be seen as a simplified problem of the rotor/stator interaction. In He's study, the rotor is treated through VLM with an unsteady wake model. The rudder is simulated through BEM. The unsteady

interaction between the wake of the rotor and the rudder is carried out straightforward. Cavities on the rudder had also been simulated and compared with experimental observation.

In this paper, the cavity model in our methods in general was first validated with the results from RANS simulation (by ANSYS Fluent). Then, effort has been made to extend He's rotor/rudder model into a rotor/stator model. Moreover, the cavitation process on the stator will be studied. A simple rotor/stator approximate the ONR AxWJ-2 water-jet pump is selected in this study. Current numerical model includes three parts: 1). a VLM unsteady rotor model; 2). A non-axisymmetric unsteady stator model with cavity model, based on low order BEM, and 3) a fully unsteady wake model which can handle the downstream blockage due to the stator blades. However, the effects of the hub and the casing are not incorporated in the current model yet.

2 FORMULATION

2.1 Cavity Model

The cavity model based on low order panel methods is described in Fine and Kinnas (1993). The cavities are modeled by putting sources on the cavitating panels of the blade. The kinematic boundary condition on the cavitating panels is used to predict the cavity height. The cavity length in the chord-wise direction of each blade strip is determined by a search algorithm which sets a cavity closure condition on the cavity height of the panel where the cavity surface re-attaches the blade. Although it is possible and necessary to include the viscous effects by coupling the current methods with a boundary layer solver, we ignore the viscous effects in the current cavity model.

2.2 Unsteady VLM model of the Rotor

Vortex Lattice Method (VLM) is adopted to model the rotor. The main framework of the rotor model is the same as that used by He (2010) in the study of unsteady propeller and rudder interaction. The governing equation of the VLM in the discretized form is written as:

$$\sum \Gamma_B \boldsymbol{v_\Gamma} \cdot \boldsymbol{n} + \sum Q_B \boldsymbol{v_Q} \cdot \boldsymbol{n} + \sum Q_C \boldsymbol{v_Q} \cdot \boldsymbol{n} + \sum \Gamma_W \boldsymbol{v_\Gamma} \cdot \boldsymbol{n} = (\boldsymbol{V}_{IN} + \boldsymbol{q}_{Stator}) \cdot \boldsymbol{n}, \quad (1)$$

where Γ_B and Γ_W denote the strength of vortices on the blade and wake. Q_B and Q_C are the strength of the line sources representing the blade and cavity thickness, respectively. $\boldsymbol{v_\Gamma}$ and $\boldsymbol{v_Q}$ are the induced velocity by unit line vortex and line source. $\boldsymbol{q}_{Stator}$ is the stator induced velocities on the control points of the rotor. Eq. (1) represents the kinematic boundary condition on the mean camber surface of the rotor blade.

Notice that Eq. (1) $\boldsymbol{V_{IN}}$ is the inflow velocity representing the upstream flow condition, which is defined under the propeller fixed coordinate system. Therefore, the velocity component due to the rotation of the rotor has to be included in $\boldsymbol{V_{IN}}$.

In order to minimize the computational cost, the periodicity of the rotor is exploited, e.g. any blade at a given blade angle has the same flow characteristics, such as bound vorticies, pressure distribution and trailing edge wake. This assumption is generally true as long as the inflow conditions under the ship fixed coordinate system are steady. With this assumption, Eq. (1) is only solved for the key blade at different blade angles. The effects of the rest blades are treated as known, by associating the surface singularities (vorticies and sources) and the trailing edge wake with those of the key blade at the corresponding blade angles. With a few revolutions, the surface singularities and also the trailing edge wake of the key blade will converge at every blade angle.

2.3 Unsteady non-axisymmetric BEM model of the Stator

Although stator does not move, it is usually subject to the wake flow downstream of the rotor. The relative motion between the rotor and the stator make the stator model intrinsically unsteady. Given the fact that the rotor and stator usually have different number of blades, the axi-symmetry is not available either, in other words, at a certain time step, the potentials and sources on a blade will not be the same as those on another. In order to handle the non-axisymmetry, at each time step, unknowns on different blades are solved respectively. The interaction between blades is included in an iterative manner, meaning the "key blade token" is looping over all the blades several turns at each time step.

The BEM model for the stator is formulated with the perturbation potential, which is defined as:

$$\boldsymbol{q} = \nabla\phi + \boldsymbol{U}_\infty + \boldsymbol{q}_{rotor}, \quad (2)$$

where $\boldsymbol{q}$ is the total velocity in the ship fixed coordinate system, $\boldsymbol{U}_\infty$ is the inflow velocity far upstream of the whole system of the rotor/stator, ϕ is the perturbation potential due to the presence of the stator, and $\boldsymbol{q}_{rotor}$ is the rotor induced velocity.

The perturbation potential satisfies the Laplace Equation:

$$\nabla^2\phi = 0, \quad (3)$$

and the slip boundary condition on the wetted surface leads to following kinematic boundary conditions:

$$\frac{\partial\phi}{\partial n} = -(\boldsymbol{U}_\infty + \boldsymbol{q}_{rotor}) \cdot \boldsymbol{n}, \quad (4)$$

where $\boldsymbol{n}$ denotes the normal vector on the surface. Applying Green's third identity, Eq. (3) written as a boundary intergral form:

$$2\pi\phi_p = \iint_{S_B}\left[\phi_p \frac{\partial G(p,p')}{\partial \boldsymbol{n}_{p'}} - \frac{\partial \phi_p}{\partial \boldsymbol{n}_{p'}} G(p,p')\right] dS + \iint_{S_W} \phi_w(y_{p'}) \frac{\partial G(p,p')}{\partial \boldsymbol{n}_{p'}} dS + \iint_{S_B} (\boldsymbol{q}_{rotor} \cdot \boldsymbol{n}) G dS, \quad (5)$$

where S_B and S_W represents the blade surface and the wake respectively, and $G(p,p') = 1/R(p;p')$ is the Green's function in 3D.

2.4 Fully Unsteady Wake Model Of The Rotor

The unsteady wake model in the study of the rotor and stator interaction plays the most critical role, because the swirl velocity due to the rotation of the rotor is mainly carried by the free wake sheets. On the other hand, the curling of the rotor wake around the stator blade creates entangled wake shape. Modeling the rotor wake is therefore a very challenging topic either in a numerical sense or in a physical sense.

The unsteady wake model in this study is improved from that originated by He (2011) in his study of propeller and rudder interaction. However, developing a wake model which can interact with a stator requires more careful numerical efforts than that with a rudder. Rudders usually have simple and straight geometry. The wake can only be cut by the rudder twice in one revolution. Also, rudders generally are large in size, so that they can tolerate more numerical errors in the geometric representation of the wake. At the meantime, the geometry of the stator is often complicatedly curved. The wake can be cut multiple times by the stator in one revolution. Comparing with the rudder, the size of the stator is often too small to bear erroneous representation of the wake geometry.

Regardless the new challenges arising from the stator, the basic idea of the wake model is the same as that proposed by He (2010):

(i). convection of the free wake.

The wake panels along with the dipole strengths are convected by the total velocities evaluated at the nodal points of the panels. In order to evaluate the total velocities, numerical evaluation of the Biot-Savart Law is required. In order to avoid unbounded velocity, the singular Biot-Savart kernel is replaced by a Rosenhead-Moore kernel (as in Ramsey 1996, Tian and Kinnas 2012). Therefore the induced velocity due to a constant dipole panel can be written as:

$$\boldsymbol{V} = \frac{\Gamma}{4\pi}\oint \frac{\boldsymbol{s}\times\boldsymbol{r}}{(r^2+\delta_K^2)^{3/2}} dl, \quad (8)$$

where δ_K is a filtering parameter, which is of the same order of the size of the panels on the wake. $\boldsymbol{s}$ is the tangential vector along the vortex loop, and $\boldsymbol{r}$ is the vector from the running point on the vortex loop to the field point.

Once the velocities on the nodal points of the wake panels are evaluated, the wake sheet is thereby convected using an Euler-Explicit scheme, as shown in Fig. 1.

(ii). Physical model of the curling of the wake.

The plain wake model presented above is largely an inviscid wake model, even though the filtering parameter δ_K carries a little sense of the viscous effects. From the theory of inviscid fluild flow, free wake sheets are material surfaces which can never been cut through by the stator blades. At the same time, the free wake sheets away from the stator blades will be continuously convected downstream. Thus the wake sheets are stretched longer and longer, and curl around the stator blades.

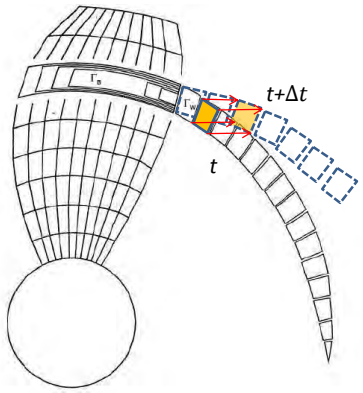

Figure 1: Schematic plot of the convection of the wake.

The curling of the tip vortex of the wake sheets were clearly observed in the experiment of propeller and rudder interaction carried in the cavitation tunnel (Karcht 1989a,b). With the presence of the stator, the curling of the wake sheets could create very complicated geometry.

In reality, the wake sheets that are blocked by the obstacles cannot last forever. Viscous effects will diffuse the stretched wake sheets rapidly. This fact actually helps us to design a numerically implementable wake model -- we could not model a wake sheet which becomes infinitely long as time goes on, but with a rational damping model of the wake, we can throw away the wake patches which have negligible effects.

He (2011) reasoned the stretching of the shed vortex on the wake surface with the viscous decay of the vorticity strength on the wake, e.g. the farther the initially neighboring points are stretched apart, the weaker the effects due to the vorticities between those two points are.

Defining the stretching ratio S_r as

$$S_r = L_0/L, \quad (9)$$

where L_0 is the arc-length along the vortex line between two nodal points before stretching, and L is the arc-length after stretching, then the effective vorticity strength after stretching is written as:

$$\Gamma_{eff} = \Gamma_M[1 - e^{c\,S_r}], \quad (10)$$

where Γ_M is the original vortex strength shed from the rotor blade, Γ_{eff} is the effective vorticity strength when evaluating the induced velocity from the wake to the stator, and c is a constant which requires calibration. Eq. (10) is formed analogously to the Lamb-Oseen vortex model. The physical consideration behind Eq. (10) is explained by He (2010).

The model described in Eq. (10) could be an oversimplification. But further improvement requires more experimental or numerical investigation in order to understand the physical process clearer. In this study, the wake panels are removed if S_r is less than 0.02, and the effects of these panels on the rotor will not be evaluated. In order to avoid inaccurate stator induced velocity close to the stator surface, a numerical clearance is set to keep the wake panels always away from the stator surface.

2.5 Modeling the Interaction

Eq. (1) and Eq. (5) both have interaction terms containing $\boldsymbol{q}_{stator}$ and $\boldsymbol{q}_{rotor}$. The interaction is handle in a iterative manner, as shown in Fig. 2.

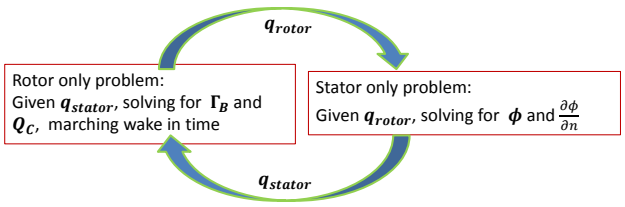

Figure 2: Iterative approach of solving the interaction problem.

Given an approximate $\boldsymbol{q}_{stator}$, we can solve the rotor only problem, and obtain an approximate $\boldsymbol{q}_{rotor}$. With the $\boldsymbol{q}_{rotor}$, the stator only problem can be solved for more accurate q_{stator}, and so on so forth. From the computational point of view, the iterative approach seems to be more efficient.

3 RESULTS AND DISCUSSION

3.1 Validation of the Cavity Model

In order to validate the cavity model in our methods, simulations through RANS and also the BEM were performed for propeller NSRDC 4381, which is a 5 bladed propeller and was investigated by Boswell (1971). The cavitation number $\sigma_n = (P_\infty - P_v)/0.5\rho n^2 D^2$ for both cases was 2.3, and the advance ratio $J_s = V_s/nD$ for both cases was 0.6, where P_∞ and P_v are operating pressure and vapor pressure respectively, ρ is the density of water, n is the rotational velocity of the propeller in RPS(revolution per second), D is the diameter of the propeller, and V_s is the ship speed.

In the RANS simulation, 1.8 million hexahedral cells were used to mesh 1/5 of the domain, as shown in Fig. 3. $k-\omega$ SST turbulence model was adopted. In order to model the cavitation process, the two-phase fluid mixture model and the Schnerr-Sauer cavitation model were selected. The wall y^+ was controlled below 15. During the simulation, efforts had been taken to lower the operating pressure gradually to approach the desired cavitation number, so that the RANS solver did not run into initial conditions which would cause divergence. The total wall time for the RANS simulation was about 8 hours on 24 Intel Xeon 2.50GHz cores.

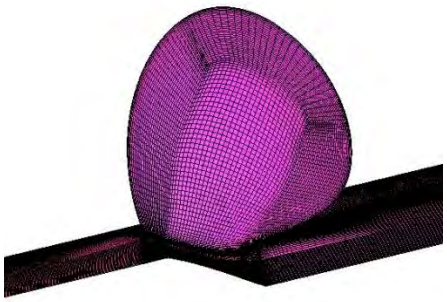

Figure 3: RANS grid on the blade and hub of propeller NSRDC 4381.

For the BEM simulation, 60×20(chordwise×spanwise) panels were used to resolve the blade surface. It took about 1 minute on a single core of the same type CPU as that in the RANS case to complete the run.

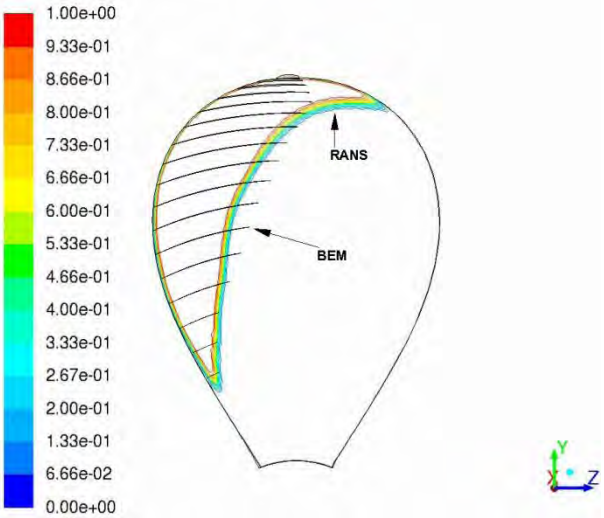

Figure 4: Comparison of the cavity patterns between the results from RANS and BEM.

Fig. 4 compares the cavity patterns predicted by RANS and BEM. The color contour shows the distribution of the volume phase fraction of the vapor over water. The results from both methods agree largely well with each other. The slight overshot of the cavity length by the BEM could be related to the lack of viscous effects. Without viscosity, the pressure rises significantly at the ending of the cavity due to the local stagnation point effect of converging flow. The pressure rise can be re-confirmed by looking at the detailed comparisons of pressure distribution, as shown in Fig. 5.

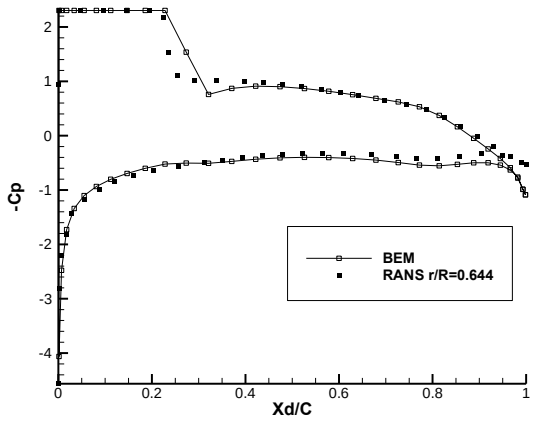

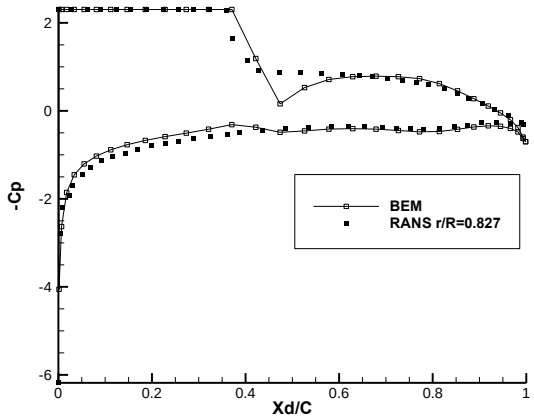

Figure 5: Comparisons of the pressure distributions predicted by RANS and the BEM at different blade strips.

In Fig. 5, two radial strips (r/R=0.644 and 0.827) were selected to compare the pressure distribution. Obviously, both methods were able to recover the vapor pressure in the cavitating parts of the blade sections. The results are also consistent in most of the wetted parts. However, discrepancy can be found in the transitional regions between cavity and fully wetted surface. The BEM results show more drastic variation in pressure in such regions than the results from RANS. The authors believe that coupling the current BEM cavity model with a boundary layer solver will bring the results closer to those from RANS.

3.2 Rotor and Stator Interaction

The present method is applied to a test stator and rotor system. At this stage, no hub nor casing model are applied. The stator geometry has similar geometric parameters as those of the stator of the ONR AxWJ-2 water-jet pump (Michael et al. 2008). The stator blade in this study does not have any contraction of the passage. The root radius of this stator is set as 0.42R.

The rotor used in this study has similar pitch angles as those of the ONR AxWJ-2 rotor, the design advance ratio J_s of this rotor is 1.2. The stator and rotor geometry are shown in Fig. 3. Numerical simulation of this propulsion system at $J_s = 1.2$ is carried out. The time step size for this simulation is set as 5degree.

Figure 6: Geometry of the test rotor and stator system.

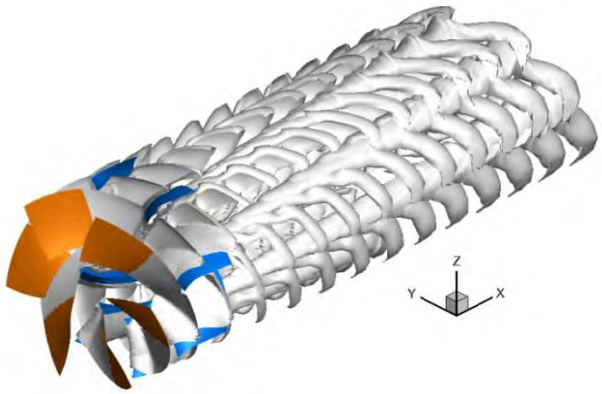

Figure 7: Geometry of the wake at the 12th revolution of simulation.

Fig. 7 shows the wake geometry at the 12th revolution of simulation. The wake is definitely twisted due to the presence of the stator, but visually reasonable. Fig. 8 renders the stretching ratio of the wake shed from a single blade. Clearly we can observe the curling and stretching of the wake. It is also interesting that as the wake sheet is elongated in the stream-wise direction it turns to shrink in the radial direction.

Fig. 9 and Fig. 10 compare the unsteady thrust coefficient (KT) and torque coefficient (KQ) of a single blade of the rotor at different blade angles with those of the steady rotor only case. The forces are converged at the 3rd iteration. Strong periodicity appears in the forces history. The thrust output from the rotor seems to be improved due to the presence of the stator. This is consistent with our expectation, although the amount of improvement may seem to be too much. This may relate to the method to evaluation of the forces. Careful investigation has to be planned in order to understand how to correctly apply the Bernoulli's equation and Joukowski law when the stator

* Leave blank the last 2.0 cm on the first page to place some additional informational about this paper in a footnote on the first page if necessary.

induced velocity comes to play.

Fig. 11 and Fig. 12 show the KT and KQ on a single blade of the stator. The forces converge at the 4th iteration. Again, we observed periodicity, which is consistent with the number of blades of the rotor.

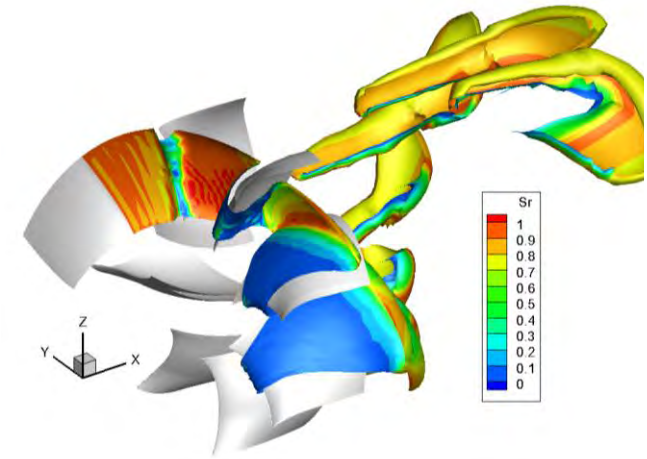

Figure 8: Stretching ratio on the wake surface.

After the fully wetted simulation getting converged, a simulation of the unsteady cavitation of the stator is carried out using the same rotor induced velocities as those from the wetted simulation. Because this propulsion system is only for preliminary test of the current numerical models, the propulsion system is not carefully designed and the stator is working under an off-design condition, which gives negative loadings near the leading edge of the stator. Consequently face side cavities are predicted, as shown in Fig. 13. The σ_v in this case is selected as 1.25.

Fig. 14 shows the cavity volume on the first blade of the stator, when the key blade of the rotor is at different blade angles. Again, we find periodicity, which is consistent with the number of blades of the rotor, although the cavity volume seems not to be smooth. The authors believe that in order to resolve the narrow range of the angles in which the trailing edge of the rotor passes the leading edge of the stator, smaller time step size is required. This will be planned after further validations of the fully wetted code.

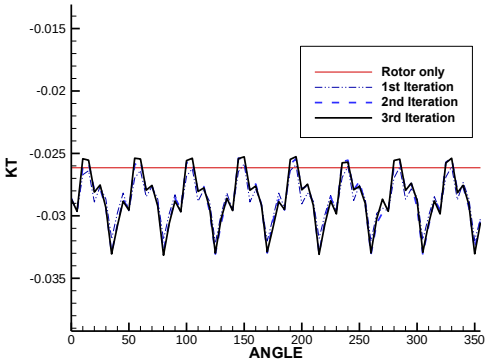

Figure 9: Convergence of single blade KT of the Rotor.

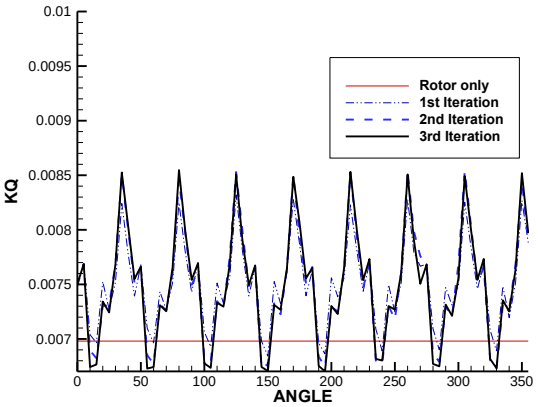

Figure 10: Convergence of single blade KQ of the Rotor.

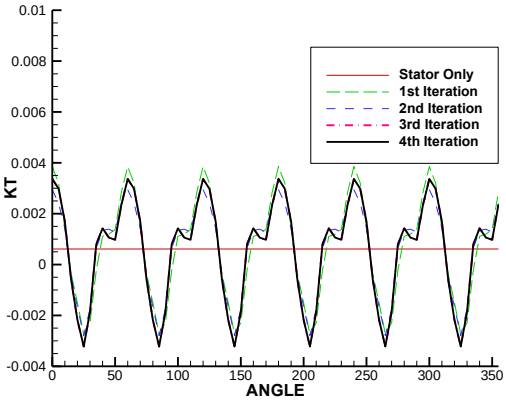

Figure 11: Convergence of single blade KT of the Stator.

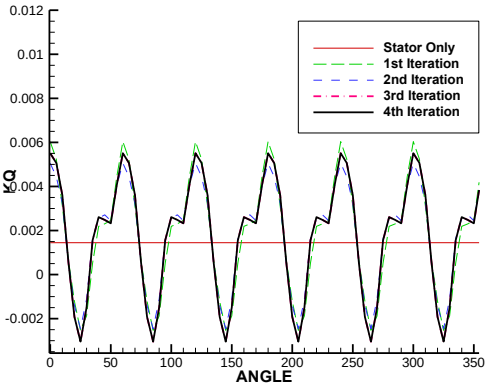

Figure 12: Convergence of single blade KQ of the Stator.

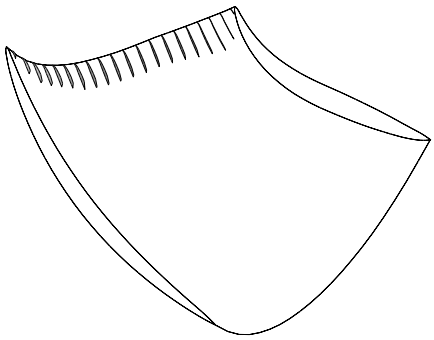

Figure 13: Cavity patterns on the 1st blade of the Stator, when the key blade of the rotor is at 0DEG of blade angle.

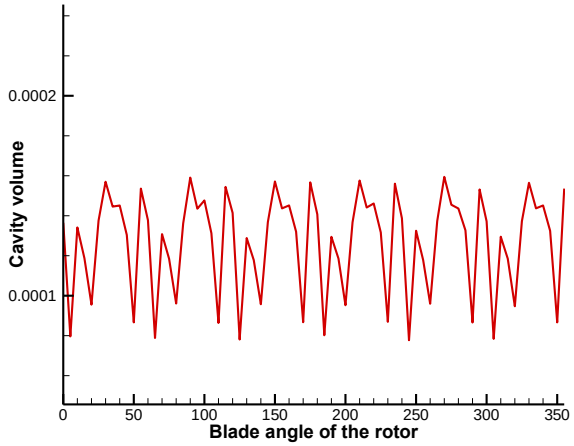

Figure 14: Cavity volume on the Stator.

4 CONCLUSIONS AND FUTURE WORK

A fully unsteady model to simulate the unsteady cavitating interactions of the rotor and stator propulsion system was proposed and implemented.

The cavity model in current methods was first validated against the results from RANS simulation with cavitation model based on two-phase mixture flow. Although the cavity model in current methods slightly over-predicted the cavity length compared with RANS, the results from both methods agreed largely well. The results from current methods can still be improved by coupling with a boundary layer solver to take account the viscous effects.

Preliminary application of the current model was then carried out on a test rotor and stator propulsion system. Unsteady and periodic forces histories were observed. The presence of the stator increased the thrust provided by the rotor. A simulation of the unsteady cavitation of the stator was also performed. The predicted cavity patterns were reasonable. The cavity volume behaved periodically consistent with the number of blades of the rotor as well.

The results for the rotor and stator interaction presented in this paper are preliminary. The unsteady wake model, and also the information passing interface between the rotor code and the stator code require careful validations. Further investigation will be conducted to include the hub and casing into the current model, so that the current model can be correlated with available experimental measurements.

ACKNOWLEDGMENTS

Support for this research was provided by the U.S. Office of Naval Research (Contract N00014-07-1-0616) and Phases VI of the "Consortium on Cavitation Performance of High Speed Propulsors" with the following current members: American Bureau of Shipping, Kawasaki Heavy Industry Ltd., Rolls-Royce Marine AB, Rolls-Royce Marine AS, SSPA AB, Andritz Hydro GmbH, Wärtsilä Netherlands B.V., Wärtsilä Norway AS, Wärtsilä Lips Defense S.A.S., and Wärtsilä CME Zhenjiang Propeller Co. Ltd.

REFERENCES

Boswell, R.J. (1971). Design, Cavitation Performance, and Open-Water Performance of a Series of Research – Skewed Propellers. Naval ship research and development center. Department of the Navy.

Brewton, S., Gowing, S., and Gorski, S. (2006), "Performance Predictions of a Water-jet Rotor and Rotor/Stator Combination Using RANS Calculations," Proc. 26th Symposium on Naval Hydrodynamics, Rome, Italy.

Chun, H. H., Park, W. G., and Jun, J. G. (2002), "Experimental and CFD Analysis for Rotor-Stator Interaction of a Water-jet Pump," Proc. 24th Symposium on Naval Hydrodynamics, Fukuoka, Japan, 744-7

Chesnakas, C. J., Donnelly, M. J., Pfitsch, D. W., Becnel, A. J., and Schroeder, S. D. (2009), "Performance Evaluation of the ONR Axial Water-jet 2 (AxWJ-2)," NSWCCD-50-TR-2009/089 Report, Naval Surface War-fare Center, West Bethesda, Maryland, United States.

Fine, N. E., and Kinnas, S. A. (1993), "A Boundary-Element Method for the Analysis of the Flow around 3-D Cavitating Hydrofoils," J. Ship Res., 37(3), 213-224.

He, L. (2010) "Numerical Simulation of Unsteady Rotor/Stator Interaction and Application to Propeller/Rudder Combination" PHD dissertation, CAEE, UT Austin.

Kerwin, J. E., Michael, T. J., and S. K., N. (2006), "Improved Algorithms for the Design/Analysis of Multi-Component Complex Propulsors," Proc. Society of Naval Architects and Marine Engineers Propeller/ Shafting '06 Symposium, Williamsburg, VA, United States.

Kinnas, S. A., Lee, H., Michael, T. J., and Sun, H. (2007a), "Prediction of Cavitating Water-jet Propulsor Performance Using a Boundary Element Method," Proc. of 9th International Conference on Numerical Ship Hydrodynamics, Ann Arbor, Michigan, United States.

Kinnas, S. A., Lee, H., Sun, H., and He, L. (2007b), "Performance Prediction of Single or Multi-Component Propulsors Using Coupled Viscous/Inviscid Methods," Proc. of 10th International Symposium on the Practical Design of Ships and other Floating Structures, PRADS2007, Houston, TX, United States.

Kinnas, S. A., Chang, S.-H., and Yu, Y.-H. (2010), "Prediction of Wetted and Cavitating Performance of Water-jets," Proc. of 28th Symposium on Naval Hydrodynamics, Pasadena, CA, United States.

Kracht, A. M. (1989). "Rudder in the slipstream of a propeller". Proc. of International Symposium on Ship Resistance and Powering Performance, Shanghai, China.

Lindau, J. W., Moody, W. L., Kinzel, M. P., Dreyer, J. J.,

Kunz, R. F., and Paterson, E. G. 2009, "Computation of Cavitating Flow through Marine Propulsors," Proc. of 1st International Symposium on Marine Propulsors, Trondheim, Norway, 168-177.

Lindau, J. W., Pena, C., Baker, W. J., Dreyer, J. J., Moody, W. L., Kunz, R. F., and Paterson, E. G. 2011, "Modeling of Cavitating Flow through Waterjet Propulsors," Proc. of 2nd International Symposium on Marine Propulsors, Hamburg, Germany, 142-151.

Michael, T. J., Schroeder S. D. and Becnel A. J. (2008), "Design of the ONR AxWJ-2 Axial Flow Water Jet Pump," NSWCCD-50-TR-2008/066 Report, Naval Surface War-fare Center, West Bethesda, Maryland, United States.

Ramsey, W. D. (1996). Boundary Integral Methods for Lifting Bodies with Vortex Wakes. PH.D dissertation, MIT.

Taylor, T. E., Kerwin, J. E., and Scherer, J. O. (1998), "Water-jet Pump Design and Analysis Using a Coupled Lifting-Surface and RANS Procedure," Proc. of International Conference on Water-jet Propulsion, The Royal Institution of Naval Architects, London, United Kingdom

Tian, Y. and Kinnas, S. A. (2012), "A Wake Model for the Prediction of Propeller Performance at Low Advance Ratios", International Journal of Rotating Machinery, special issue: Marine Propulsors and Current Turbines: State of the Art and Current Challenges.